



Fermi National Accelerator Laboratory

FERMILAB-Conf-86/65-E
7180.557

HADRON-NUCLEUS INTERACTIONS AT HIGH ENERGY*

R. Gomez

California Institute of Technology, Pasadena, CA 91125 USA

L. Dauwe, H. Haggerty, E. Malamud, and M. Nikolic
Fermi National Accelerator Laboratory, Batavia, IL 60510 USA

J. Lannutti, S. Hagopian, and B. Pifer
Florida State University, Tallahassee, FL 32306 USA

R. Abrams, J. Ares, H. Goldberg, C. Halliwell,† S. Margulies, D. McLeod,
A. Salminen, J. Solomon, and G. Wu
University of Illinois at Chicago, Chicago, IL 60680 USA

R. Crittenden, P. Draper, A. Dzierba, R. Heinz, J. Krider,
T. Marshall, J. Martin, A. Sambamurti, P. Smith, A. Snyder,
C. Stewart, T. Sulanke, and A. Zieminski
Indiana University, Bloomington, IN 47405 USA

R. Ellsworth
George Mason University, Fairfax, VA 22030 USA

R. Glasser, J. Goodman, S. Gupta, and G. Yodh
University of Maryland, College Park, MD 20742 USA

T. Watts
Rutgers, the State University, Piscataway, NJ 08854 USA

V. Abramov, Yu. Antipov, B. Baldin, S. Denisov, V. Glebov,
Yu. Gorin, V. Kryshkin, S. Petrukhin, S. Polovnikov, and V. Sulayev
Institute of High Energy Physics, Serpukhov, USSR

Fermilab E-557 Collaboration

May 1986

*Presented at the Second International Workshop on Local Equilibrium in Strong Interaction Physics, Santa Fe, New Mexico, April 9-12, 1986.

†Presenter

HADRON-NUCLEUS INTERACTIONS AT HIGH ENERGY

R. Gomez
California Institute of Technology
Pasadena, CA 91125

L. Dauwe, H. Haggerty, E. Malamud, M. Nikolic
Fermilab
Batavia, IL 60510

J. Lanutti, S. Hagopian, B. Pifer
Florida State University
Tallahassee, FL 32306

R. Abrams, J. Ares, H. Goldberg, C. Halliwell, S. Margulies,
D. McLeod, A. Salminen, J. Solomon, G. Wu
University of Illinois at Chicago
Chicago, IL 60680

R. Crittenden, P. Draper, A. Dzierba, R. Heinz, J. Krider,
T. Marshall, J. Martin, A. Sambamurti, P. Smith, A. Snyder,
C. Stewart, T. Sulanke, A. Zieminski
Indiana University
Bloomington, IN 47405

R. Ellsworth
George Mason University
Fairfax, VA 22030

R. Glasser, J. Goodman, S. Gupta, G. Yodh
University of Maryland
College Park, MD 20742

T. Watts
Rutgers University
Piscataway, NJ 08854

V. Abramov, Yu. Antipov, B. Baldin, S. Denisov, V. Glebov,
Yu. Gorin, V. Kryshkin, S. Petrukhin, S. Polovnikov, V. Sulayev
Institute of High Energy Physics
Serpuukhov, USSR

Fermilab E557 Collaboration

paper presented by C. Halliwell at the Second International
Workshop on Local Equilibrium in Strong Interaction Physics in
Santa Fe, New Mexico, USA, April 9 to 12, 1986.

HADRON-NUCLEUS INTERACTIONS AT HIGH ENERGY

Caltech-Fermilab-Florida-Illinois-Indiana-
George Mason-Maryland-Rutgers-Serpukhov

E557 Collaboration

Properties of energetic secondaries produced at large angles using 800 GeV incident protons are presented. H_2 , Be, C, Al, Cu and Pb targets were used for the study. The yields for producing such secondaries vary as A^α where A is the atomic mass number of the target and α attains values as large as 1.6. There is evidence that jet-like events have α values approaching unity, indicating a hard scattering mechanism may be occurring. Events with large values of target-fragmentation energy have, on average, large values of energy in the central region and small values of forward-going energy. Energy flows and number of secondaries are independent of the target when events with similar amounts of energy in the central region are studied.

INTRODUCTION

Interactions of hadrons with nuclei (hA interactions) have been studied in the past primarily to investigate the production and subsequent space-time evolution of the produced secondaries¹⁾. This has been possible because the nucleus interferes with the secondaries immediately after the primary interaction, an occurrence that cannot take place in hadron-nucleon (hN) interactions.

From these hA studies it has been found that low energy secondaries, produced mostly in the target-fragmentation region, are formed inside the nucleus and therefore cascade within the nucleus causing a multiplicity enhancement when compared to data from hN interactions. In contrast to this, the average number of secondaries formed in the central region is approximately proportional to the average number of collisions expected within a nucleus²⁾. This result has led to the idea that energetic secondaries are produced outside of the nucleus and therefore are unable to take part in a hadronic cascade. Finally, leading particles from hA interactions have less energy compared to those produced in hN

interactions because of momentum degradation caused by collisions within the nucleus³⁾

Recently, interest has focussed on the production of leading hadrons from hA interactions. By measuring the energy lost by the incident hadron, it is hoped that an estimate can be made of the energy deposited within the nucleus. This in turn may be useful in estimating the incident hadron energies required to study the formation of the quark-gluon plasma⁴⁾. An analysis⁵⁾ using this approach has been carried out recently using data from an experiment that triggered on leading particles⁶⁾.

An alternative method for studying energy deposited in the nucleus is to directly measure the energy associated with secondaries produced in the central region. This method was used in Fermilab experiment E557 which was designed to trigger on large amounts of energy at wide angles (in the vicinity of 90° as measured in the proton-proton centre-of-mass frame) to the incident beam direction ("transverse energy", E_t). One of the aims of E557 was to measure the momentum distribution of the secondaries as a function of polar angle⁷⁾. A large enhancement of positive charged particles (as compared to negative ones) was found at small angles, corresponding to energetic leading protons. This occurred in events with small amounts of E_t . The leading proton enhancement dispersed over a larger angular region as bigger E_t values were required, signifying sizeable energy lost by the protons.

The E557 data were obtained using 400 GeV/c incident protons. The experiment concentrated on hN interactions and obtained little hA data. A more recent data collection run of E557* was carried out in 1984 using 800 GeV/c protons and several nuclear targets. One of the aims of this recent run was to study the properties of rare events that occur when the incident proton loses a large fraction of its momentum. This paper reports on the analysis of these new data.

EXPERIMENTAL METHOD

The layout of the E557 apparatus is shown in Fig. 1. The experiment was performed using the Fermilab MT beam line. The apparatus consisted of several highly segmented calorimeters that detected photons and hadronic secondaries.

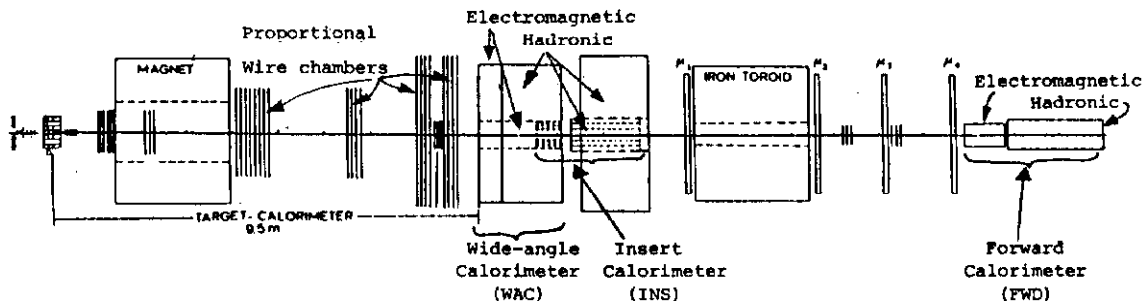


Figure 1. E557/672 apparatus at Fermilab.

The properties of these calorimeters (the wide-angle, WAC, the insert (INS), the forward, FWD, and the beam, BM) are listed in Table 1.

Table 1.

Calorimeter Properties

Calorimeter	material	acceptance		Number of modules
		in pp cm frame $\Delta\theta^*$	Δy^*	
WAC, electromagnetic	lead-scintillator	60 \rightarrow 145	-1.1 \rightarrow .5	126
WAC, hadronic	iron-scintillator	60 \rightarrow 145	-1.1 \rightarrow .5	126
INS, electromagnetic	lead-glass	22 \rightarrow 55	.7 \rightarrow 1.6	84
INS, hadronic	iron-scintillator	20 \rightarrow 50	.8 \rightarrow 1.7	24
FWD, electromagnetic	lead-glass	5 \rightarrow 30	1.3 \rightarrow 3.1	114
FWD, hadronic	iron-scintillator	5 \rightarrow 35	1.2 \rightarrow 3.1	60
BM, electromagnetic	lead-scintillator	0 \rightarrow 5	$>$ 3.1	1
BM, hadronic	iron-scintillator	0 \rightarrow 5	$>$ 3.1	1

Their segmentation and approximate acceptances, as measured in the proton-proton centre-of-mass frame, are shown in Fig. 2. The proportional wire chambers shown in Fig. 1 were not used in this analysis except for reconstructing the position of the interaction vertex upstream of the spectrometer magnet. No particle identification of the produced secondaries was attempted.

The calorimeters served as triggering devices as well as detectors of the produced secondaries. In this paper the results from two groups of triggers will be reported. Firstly, an inelastic collision was detected by demanding that a large pulse height had occurred in a counter placed immediately downstream of the target. This trigger, termed the "interacting beam" trigger, was sensitive to approximately 90% of the total inelastic proton-proton cross section. Secondly, a group of triggers consisting of the "interacting beam" trigger with an additional requirement that at least a certain amount of E_t was present in a preset region of the WAC and INS calorimeters, was also used. The modules used in the WAC and INS calorimeters to form two of these triggers are shown in Fig 3. To form the E_t triggers the output from each calorimeter module was weighted by the sine of the polar angle that the module subtended at the target. E_t sums for several different configurations of calorimeter modules were formed simultaneously. Data from three of these configurations are presented in this paper: two full azimuthal acceptance ("global", $45^\circ < \theta^* < 135^\circ$, and "limited global", $60^\circ < \theta^* < 120^\circ$) triggers and a limited azimuthal acceptance ("small aperture") trigger.

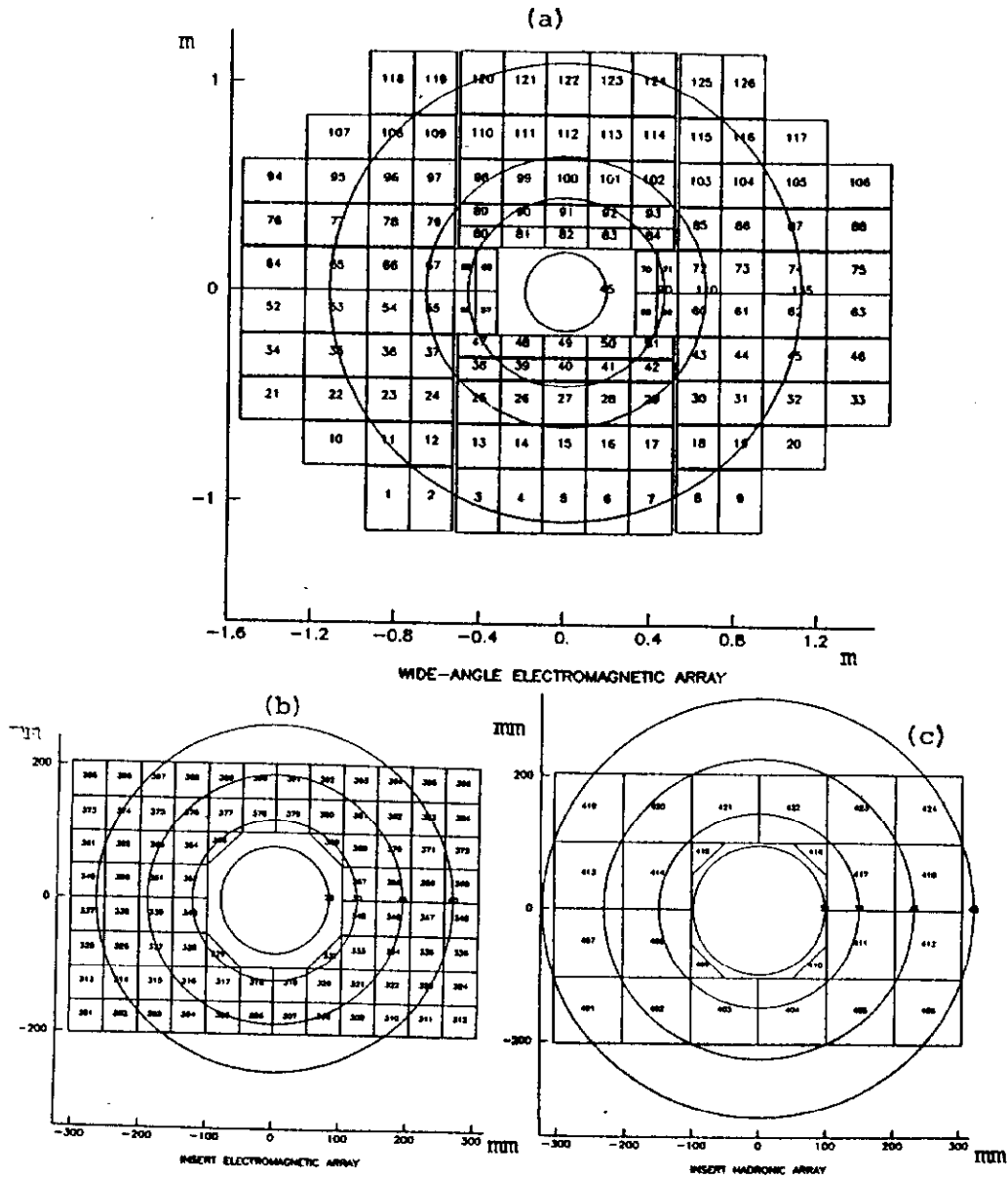


Figure 2. Segmentation and polar acceptances for massless secondaries for the (a) WAC hadronic and electromagnetic, (b) INS electromagnetic, (c) INS hadronic calorimeters. The circles are $\theta^* =$ (a) 45, 90, 110, 135, (b) 20, 30, 45, 60, (c) 20, 30, 45, 60 degrees in the proton-proton centre-of-mass frame.

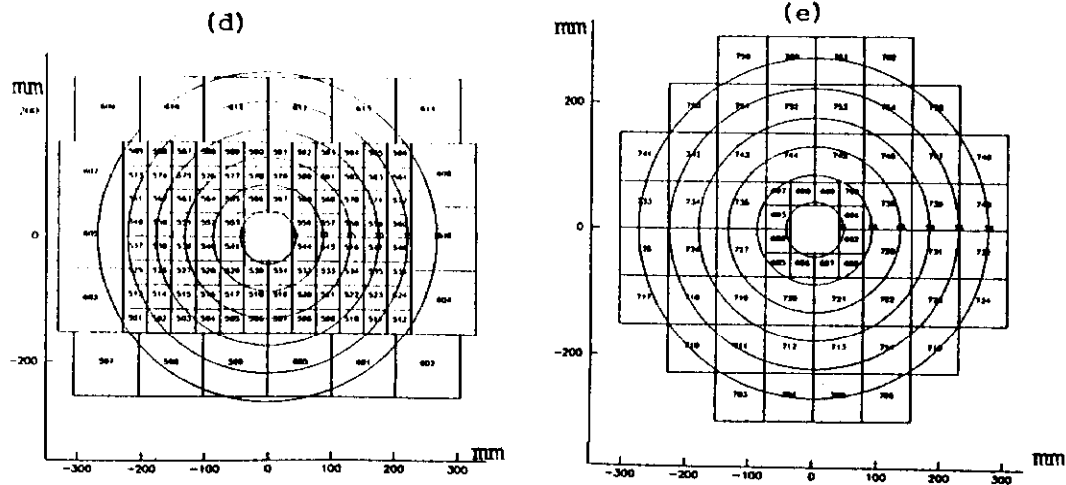


Figure 2. (cont)

Segmentation and polar acceptances for massless secondaries for the (d) FWD electromagnetic and (e) FWD hadronic calorimeters. The circles are $\theta^* =$ (d) 5, 10, 15, 20, 25, 30 and (e) 5, 10, 15, 20, 25, 30 degrees in the pp centre-of-mass frame.

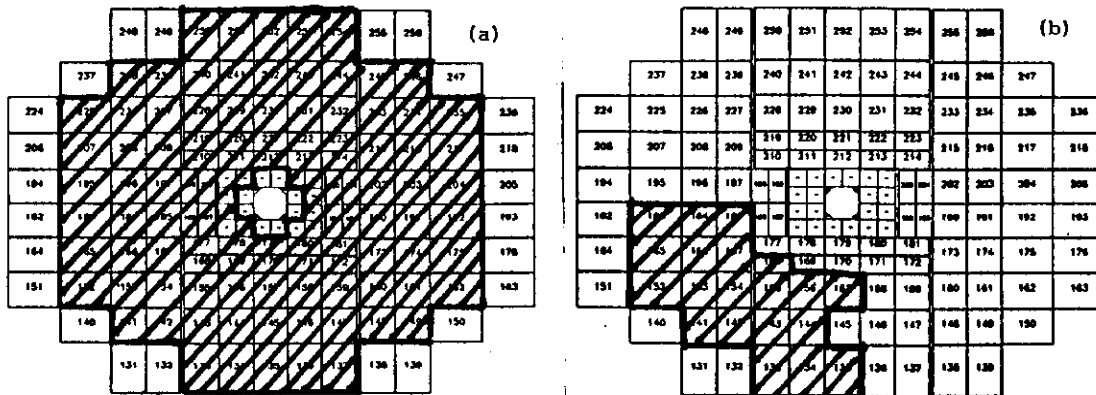


Figure 3. Modules in the WAC and INS calorimeters used to form (a) "global" and (b) a "small aperture" trigger.

ANALYSIS

The analysis presented in this paper was performed using the calorimeter module outputs directly. No correction was made for the response of the electromagnetic section of the calorimeters being approximately 20% larger for incident electrons than hadrons. It is estimated that the E_t determination has to be decreased by 17% due to this source, the p_t kick from the spectrometer magnet, the leakage from the downstream face and sides of the calorimeters and the energy resolution of the calorimeter modules. No attempt has been made to form "energy clusters" from the calorimeter data.

YIELDS

Inelastic cross sections were obtained using the "interacting beam" trigger. These cross sections were typically 10% lower than those measured in previous experiments⁸⁾. This was due mainly to the requirement that at least two charged particles had traversed the trigger counter. Yields of events with E_t values up to approximately 16 GeV as detected in the "global" trigger region (see Fig. 3) of the WAC and INS calorimeters were measured using this trigger.

Yields of events with higher E_t values were obtained by imposing an ever increasing E_t requirement from the WAC and INS calorimeters at the trigger level. By doing this it was possible to obtain events with E_t values in the "global" trigger region up to approximately 36 GeV. The results of this analysis are shown in Fig 4.

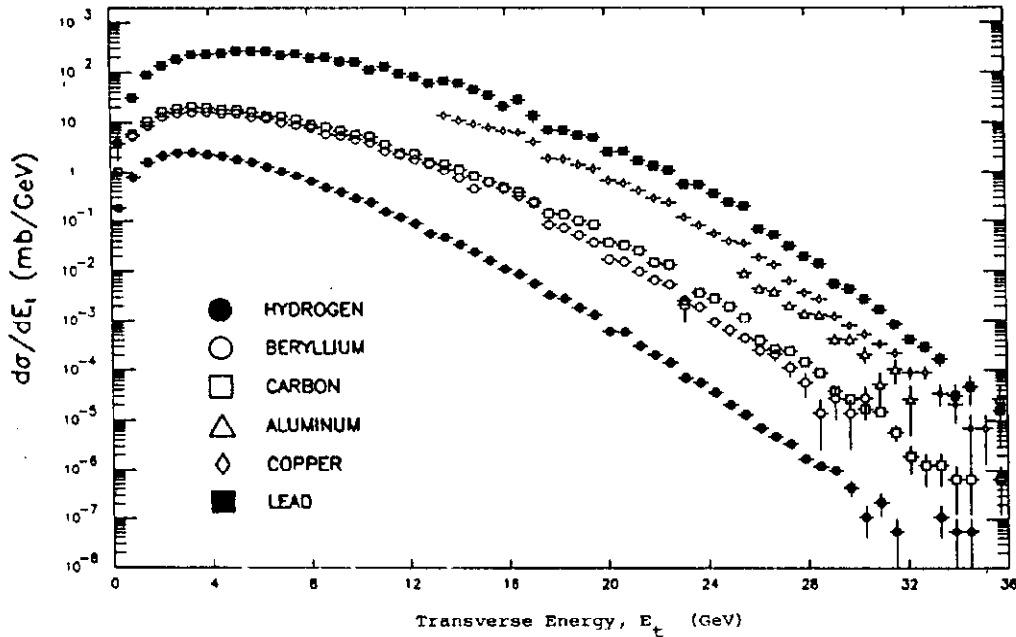


Figure 4. Yields as a function of E_t detected in the "global" triggering region. Data for hydrogen and various nuclear targets are shown. The 17% correction mentioned in the text has not been applied.

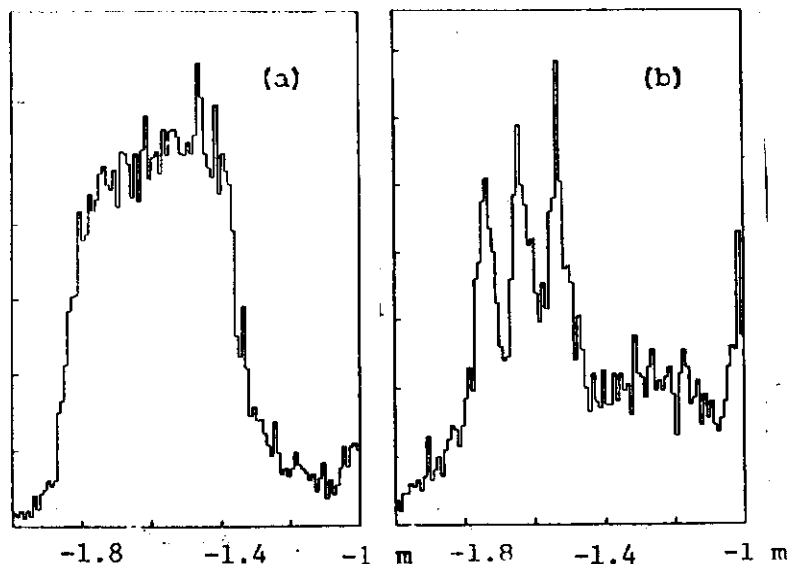
Events that contributed to this plot were required to have a reconstructed interaction vertex in the target region. The reconstruction was accurate enough to easily distinguish between the three nuclear targets (see Fig. 5). The efficiency for reconstructing vertices for events with small E_t values was somewhat lower than for events with large E_t values because the number of secondaries was typically lower for the former class of events. This inefficiency contributes to the dip in

the yield curve (Fig 4) at low values of E_t (the total inelastic cross section obtained by integrating the hydrogen data is only 16 mb).

Figure 5.

Reconstructed interaction vertex coordinate along the incident beam direction for:

(a) hydrogen and
(b) 3 lead targets.
The trigger used was "interacting beam".

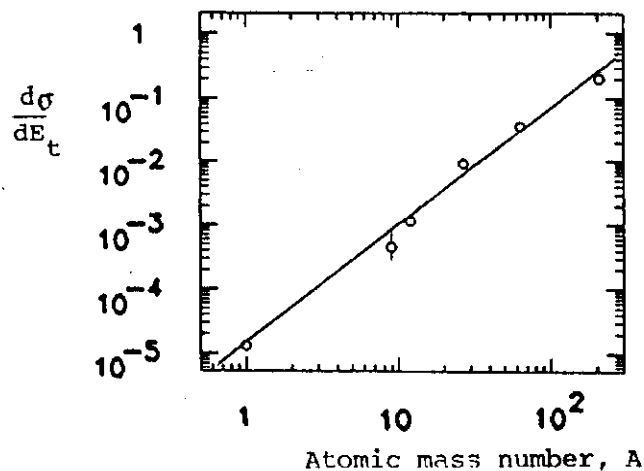


The probability of producing events with E_t values greater than, say, 32 GeV, is approximately 10^4 times greater from a lead nucleus than from hydrogen. This means that events where the incident proton loses at least 80% of its momentum (as measured in the proton-proton centre-of-mass frame) are readily accessible if nuclear targets are used.

To quantify the enhancement that nuclear targets produce compared to hydrogen, values of $d\sigma/dE_t$ for several E_t ranges for the various nuclear targets were fitted to the form $d\sigma/dE_t \propto A^{\alpha(E_t)}$. The fits did not include the hydrogen data as they typically lay well below the straight line extrapolation (see Fig. 6).

Figure 6.

Fit of $d\sigma/dE_t$ to $A^{\alpha(E_t)}$.
The E_t range was
 $25.2 < E_t < 25.8$ GeV.



The variation of α as a function of E_t is shown in Fig 7. Even if the α values for low E_t values are ignored, it is still apparent that α increases significantly above unity. This confirms similar results from other calorimeter based experiments⁹⁾ and single-particle experiments¹⁰⁾. The same trend was apparent in the "reduced global" and "small aperture" data.

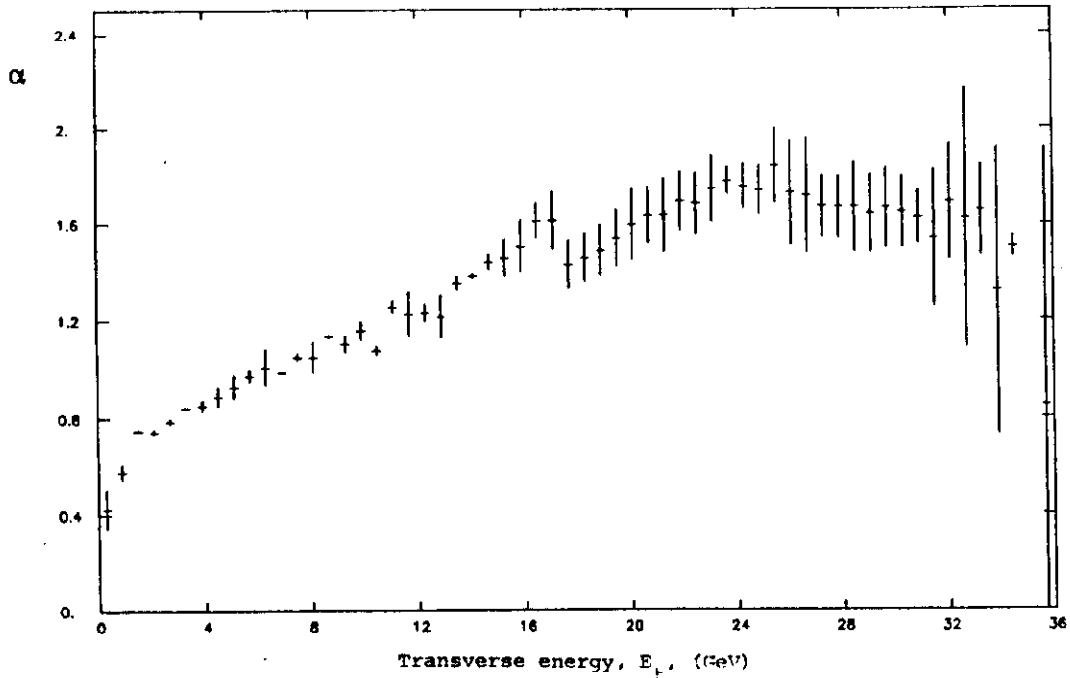


Figure 7. Variation of α with E_t detected in the "global" triggering region.

EVENT STRUCTURE

In past calorimeter experiments¹¹⁾, event structure was studied by employing the planarity variable, P . In the plane transverse to the beam direction, the principle axis of an event was found and the p_t vector for each module was decomposed into components parallel and transverse to this axis. With the sum of the squared components along and transverse to the principle axis denoted as A and B , the planarity is defined as $P = (A-B)/(A+B)$. For pencil-like back-to-back jets, P approaches 1, while for large multiplicity isotropic events it approaches 0. Fig. 8 shows the observed planarity distributions for the high E_t "global" data. Only modules that were included in the "global" triggering region contributed to the planarity calculation. It is evident from Fig. 8 that the majority of the events obtained using this trigger are nonplanar.

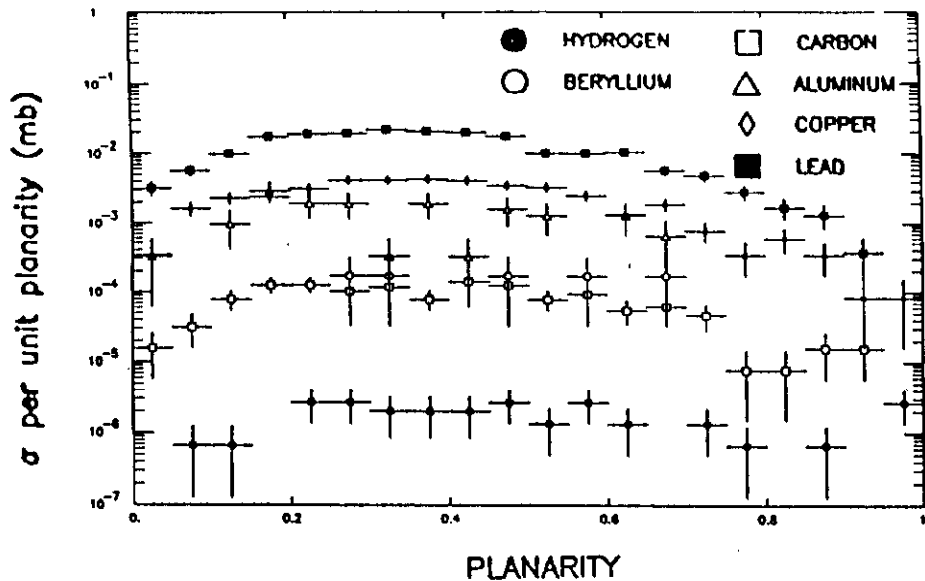


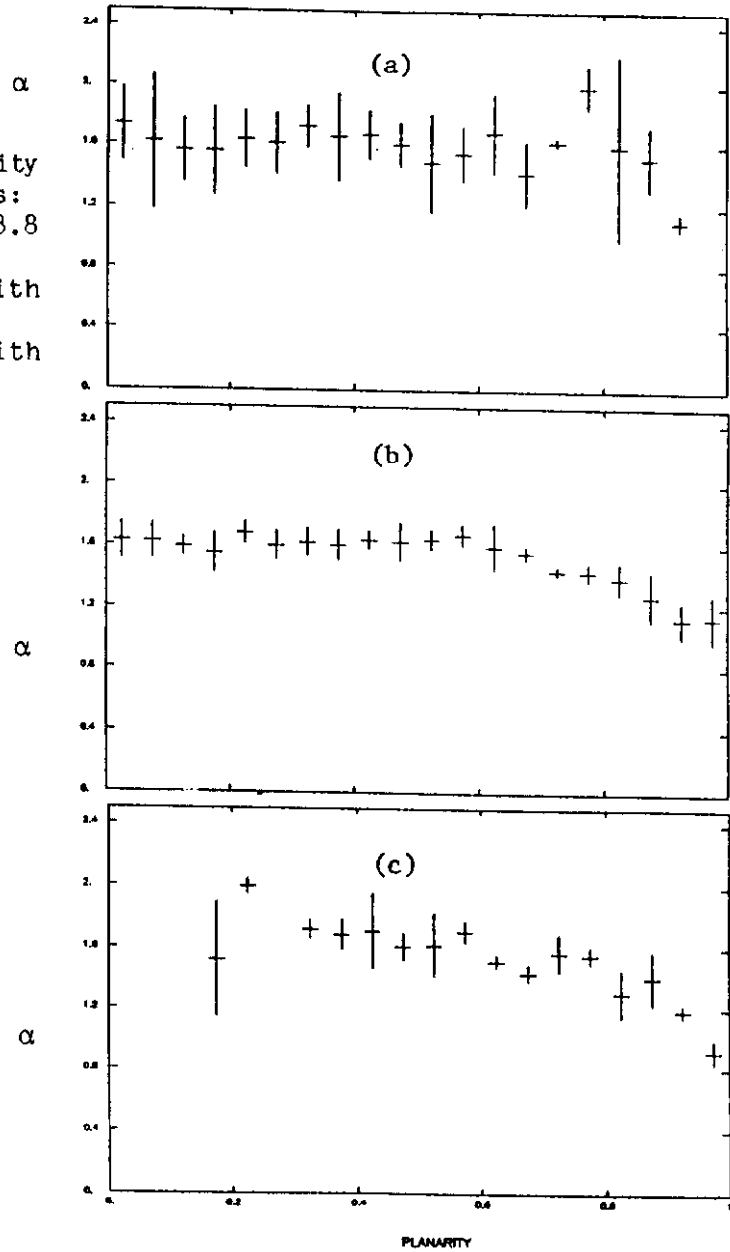
Figure 8. Planarity distributions for data collected using the "global" trigger. The E_t threshold was 28.8 GeV. Statistical errors only are shown.

The data shown in Fig. 8 can be parametrized as $A\alpha(P, E_t)$. Integrating over an E_t range, one can study how α varies with planarity. Fig. 9(a) shows such a variation for the "global" data. There is a slight tendency for α to decrease to unity from 1.6 for events with high values of planarity. This could be evidence that "jetty" events are produced by a hard scattering mechanism. This view is somewhat supported by the variation of α with planarity for the "reduced global" data (this trigger was designed to diminish the effect of forward-going secondaries being included in the scattered jets detected at wide angles) and for the "small aperture" data (see Figs. 9(b) and 9(c)). Several sets of data from various "small aperture" triggers were studied and all showed a significant decrease of α with planarity.

To see if events produced using the "small aperture" trigger are created by a different mechanism from data collected using the "global" or "interacting beam" triggers, data from a detector surrounding the target was analysed. The energy deposited in it was, hopefully, strongly correlated with the number of collisions that had occurred within the nucleus. The acceptance of the detector, as measured in the proton-proton centre-of-mass frame was $159^\circ < \theta^* < 179^\circ$. The layout of it is shown in Fig 10.

Figure 9.

Variation of α with planarity for 3 different triggers:
 (a) "global" with a 28.8 GeV threshold,
 (b) "reduced global" with a 19.1 GeV threshold,
 (c) "small aperture" with a 8.4 GeV threshold.



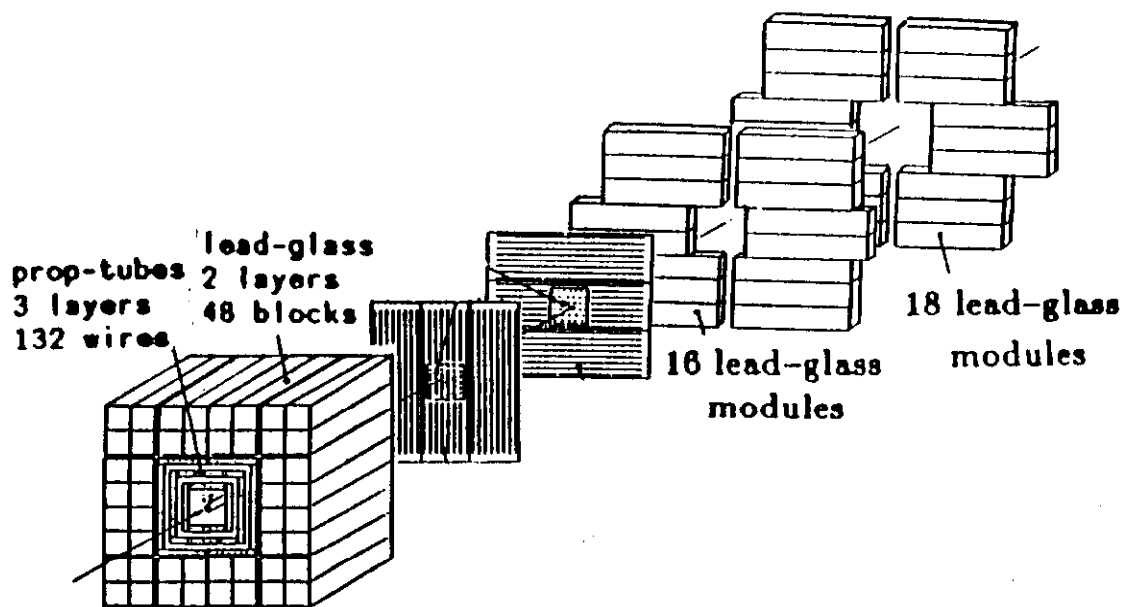


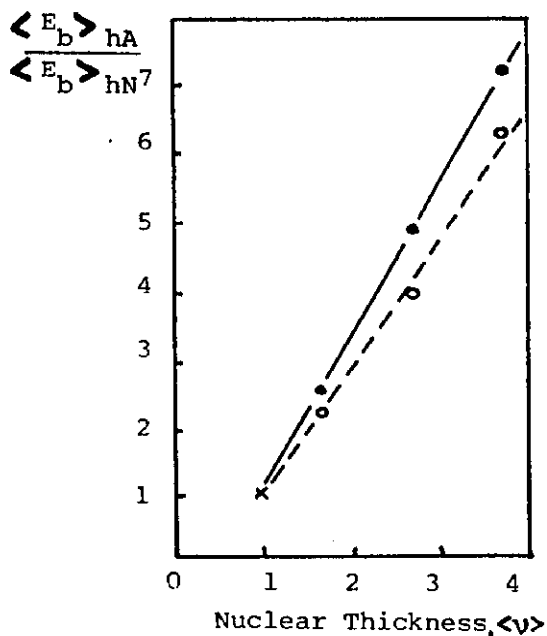
Figure 10. Exploded view of the target-fragmentation region detector.

Only data from the lead-glass blocks immediately surrounding the target (the "barrel") will be presented here.

The ratio of total energy detected in the "barrel" from hA interactions as compared to that from hN interactions is shown in Fig 11.

Figure 11.

Variation of the total energy in the "barrel" for hA interactions normalized to the total energy from hN interactions as a function of nuclear thickness, $\langle v \rangle$. $\langle v \rangle$ is defined as $A\sigma_{pN}/\sigma_{pA}$ where σ_{pN} and σ_{pA} are the total inelastic proton-nucleon and proton-nucleus cross sections and A is the number of nucleons in the nucleus. Data obtained using the "interacting beam", o, and "small aperture", ●, triggers are shown.



The enhancement of the energy in the "barrel" produced in hA interactions compared to hN ones increases faster than $\langle v \rangle$. This trend also occurs for the charged multiplicity detected in the proportional tubes surrounding the target. However, the multiplicity of secondaries is expected to increase in nuclei faster than the nuclear thickness due to the hadronic cascade within the nucleus; an increase in energy is not easily explained in naive multiple-interaction models, such as, for example, that described in Ref 12.

It was also found (see Fig. 12) that the E_t in the central region (as detected as the WAC and INS calorimeters) was linearly correlated with the average neutral target-fragmentation region energy. Also, the amount of energy detected in the "barrel" is far greater for hA interactions than for hN ones, if events with similar E_t are examined. These two observations indicate that events with large E_t values are produced by multiple interactions within the nucleus, assuming that the energy detected in the "barrel" is directly correlated with the number of collisions within the nucleus. This would add credence to the view that values of α exceeding unity are related to multiple scattering within the nucleus (see Fig. 4).

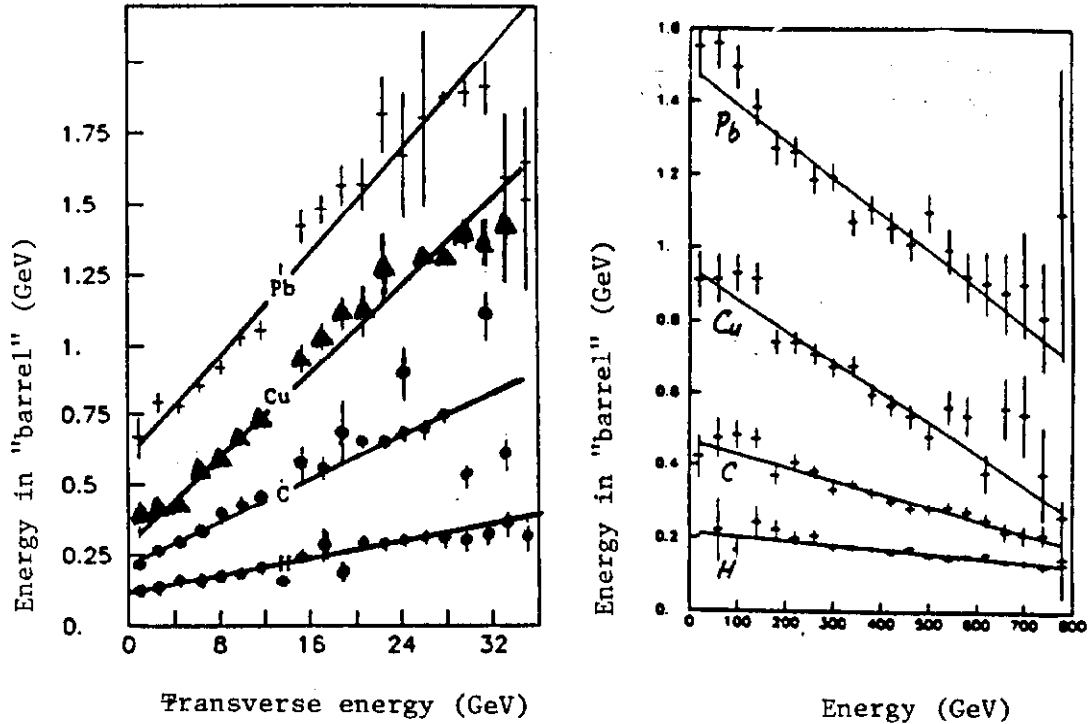


Figure 12. Correlation between energy detected in the "barrel" and (a) E_t detected in the WAC and INS calorimeters and (b) forward going energy detected in the FWD and BM calorimeters, using "interacting beam" and "global" triggers.

To see if the detailed structure of events produced in hA and hN interactions differ significantly, the energy flows (that is, average energy per event in a particular polar angular region) in the WAC, INS, FWD and BM calorimeters were combined over the angular range $\theta^* < 145^\circ$ as measured in the proton-proton centre-of-mass frame. To diminish systematic errors it has been customary in the past to divide data obtained from hA interactions by the corresponding data from hN ones. This approach could not be applied directly to the data obtained using the "interacting beam" trigger. As mentioned above, a large fraction of low E_t hN events were lost because the interaction vertex was not reconstructed efficiently. Therefore, if the hA data obtained using this trigger was divided by the corresponding hN data, a serious bias would have resulted. To overcome this problem, data from the same E_t ranges had to be compared.

In Fig. 13 comparisons of the polar angle dependence of the energy flows from hA and hN interactions are shown for events obtained using the "interacting beam" trigger. Some effects of the granularity of the calorimeters are apparent in the plots. However, it can be seen that the energy flows from hA and hN interactions are similar (to within 10%) when events with similar values of E_t are compared.

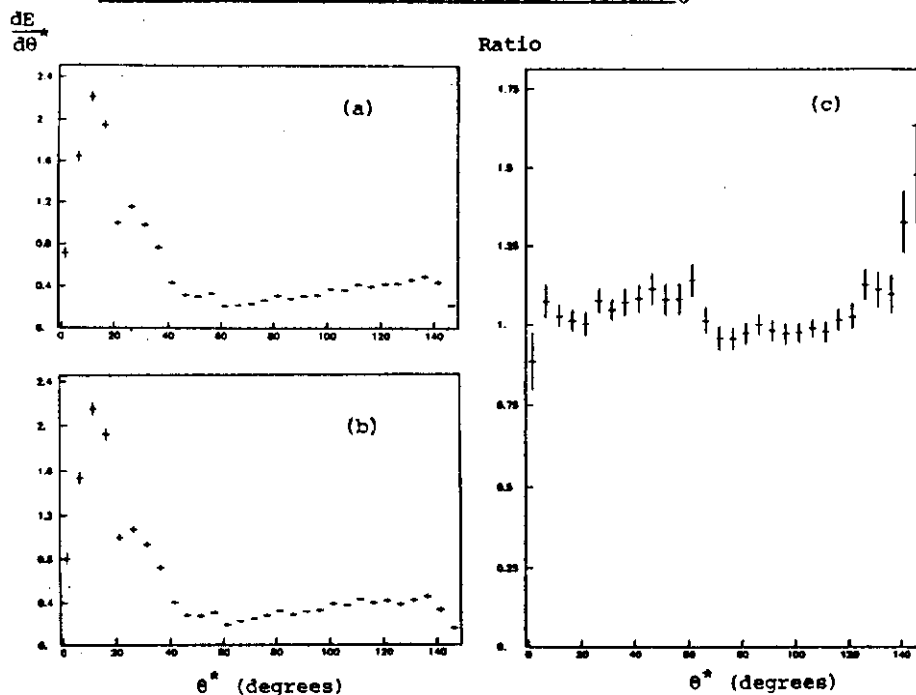


Figure 13. Polar angle dependence of energy flows (in arbitrary units) for (a) lead and (b) hydrogen data. θ^* is measured in the proton-proton centre-of-mass frame. The E_t range was $6 < E_t < 4$ GeV. E_t was measured in the "global" triggering region. (c) shows the ratio (lead/hydrogen) of the energy flows. Data from the WAC, INS and FWD calorimeters contributed to these plots.

In Fig. 15 the distributions and their ratios are shown. It can be seen that the events from hA and hN interactions have a similar number of modules firing for events with similar E_t . The data shown in Fig. 15 was obtained using an "interacting beam" trigger. Fig. 16 shows similar data using the "global" trigger with a high E_t threshold. Although the distributions for higher E_t events are broader, signifying an increase in the transverse momentum per secondary, the structure of the lead and hydrogen events remains similar.

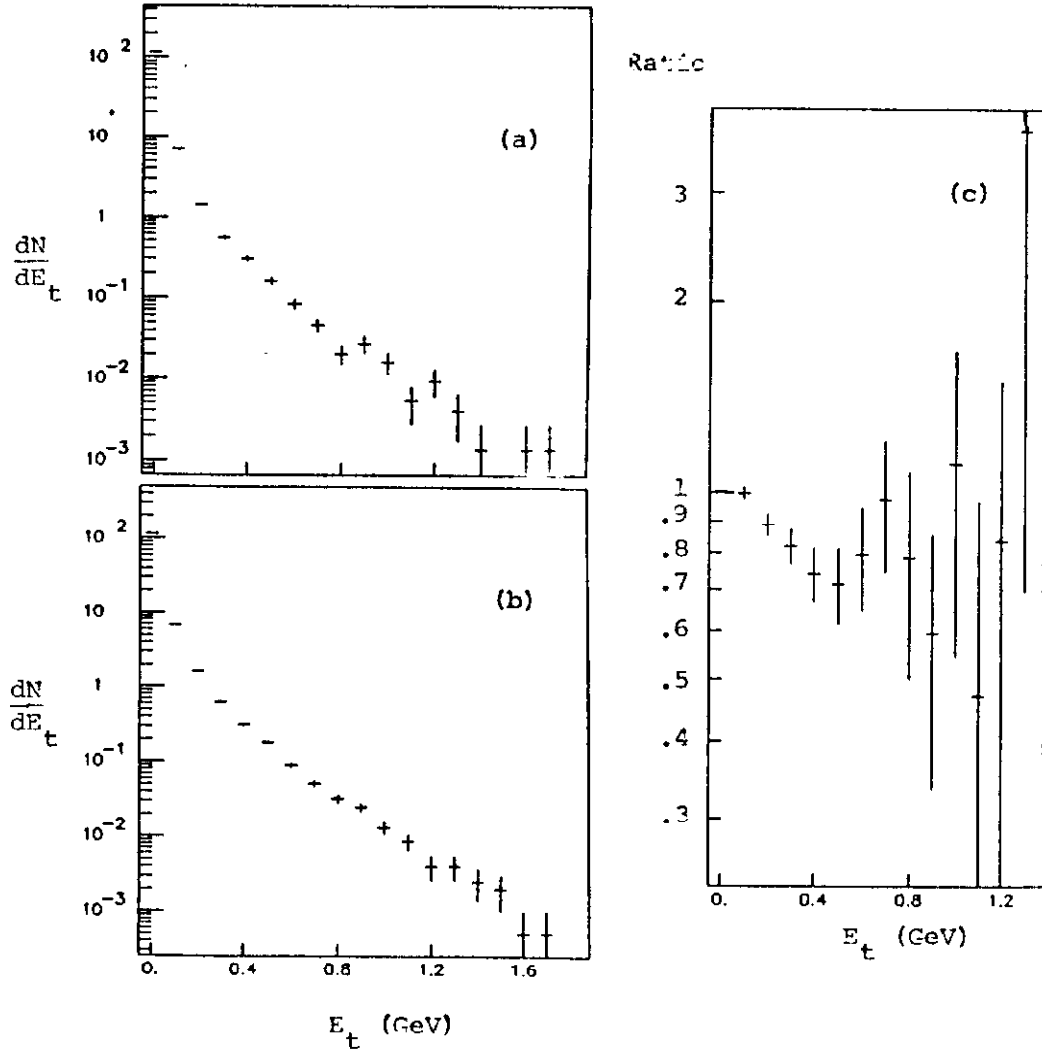


Figure 15. Average number of modules in the hadronic portion of the WAC calorimeter having E_t deposited in them for (a) lead and (b) hydrogen targets. The integral under the separate histograms is the total number of modules in the WAC, that is, 126. (c) shows the ratio of the lead to hydrogen data. The total E_t in the "global" triggering region was in the range $3 < E_t < 4$ GeV.

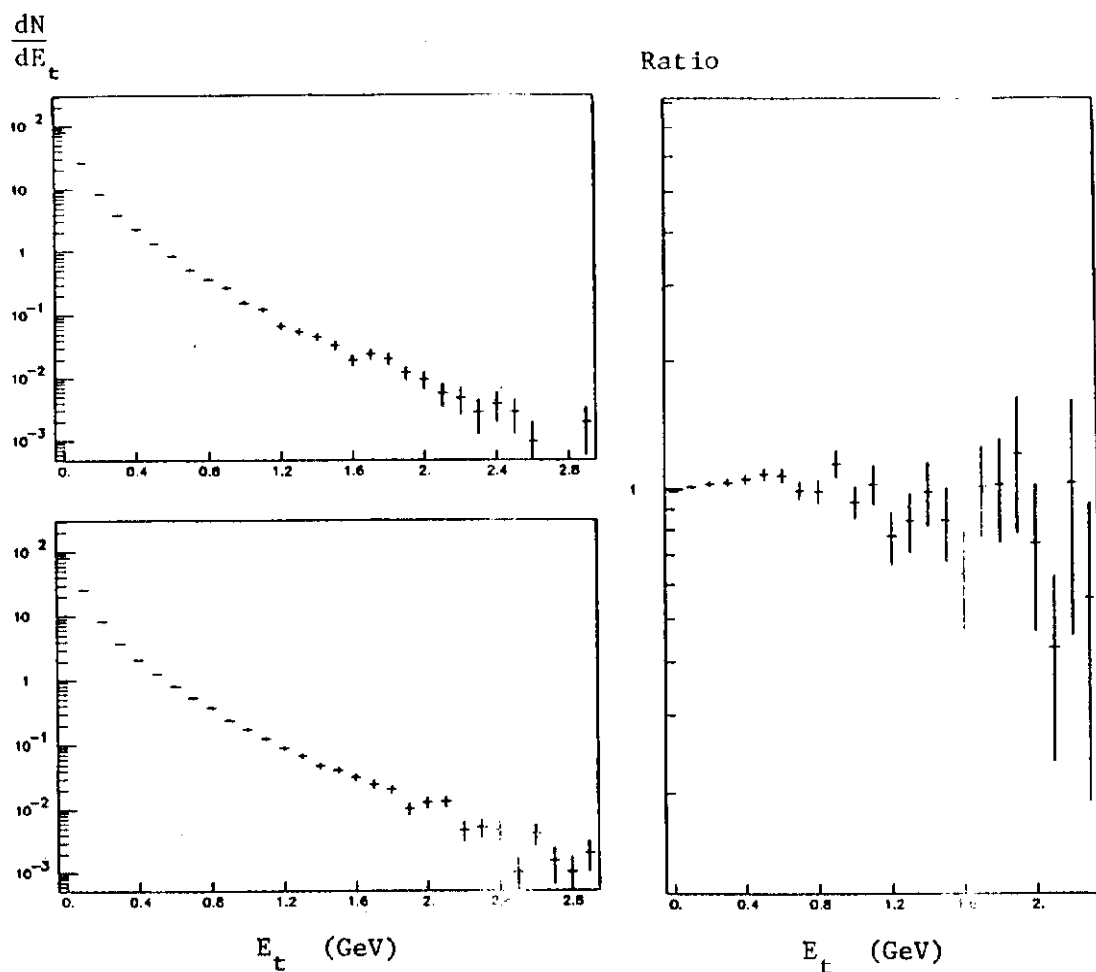


Figure 16. Average number of modules in the hadronic portion of the WAC calorimeter having E_t deposited in them for (a) lead and (b) hydrogen targets. (c) shows the ratio of the lead to hydrogen data. The total E_t in the "global" triggering region of the WAC and INS calorimeters was in the range $16 < E_t < 18$ GeV

Several previous experiments have measured the multiplicity of secondaries in the central region from hA and hN interactions. The average multiplicity from proton-lead collisions is 2 to 2.5 times that from proton-proton. The results mentioned above are not in contradiction to these previous measurements. The new results are quoted for events with similar E_t values. The average E_t value for a proton-lead interaction is approximately twice that from a proton-proton one (see the yield curves in Fig. 4). Therefore, because the multiplicity of modules with substantial E_t increases linearly with E_t as measured in the

"global" triggering region (see Fig. 17), the average multiplicity from lead is approximately twice that from hydrogen.

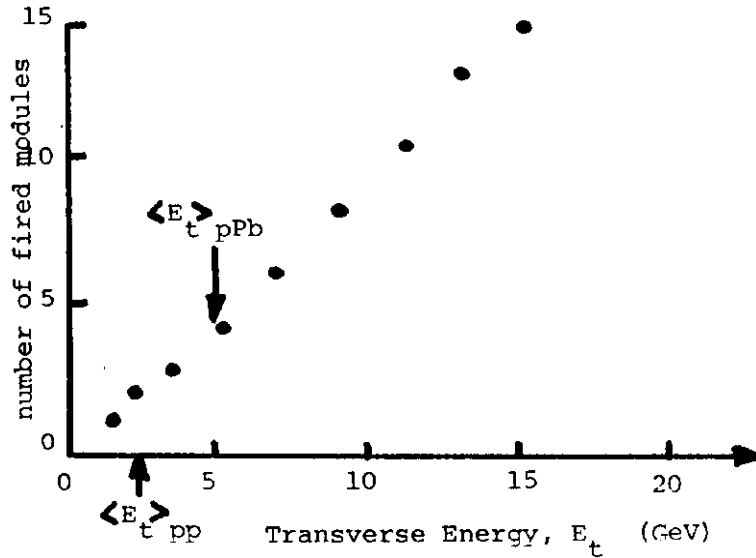


Figure 17. The multiplicity of modules in the hadronic portion of the WAC calorimeter having E_t values greater than 50 MeV in them. The data is for a hydrogen target. Similar results were obtained for proton-lead events. The value of the slope of the straight line was not sensitive to the 50 MeV E_t requirement; cuts of upto 250 MeV on module E_t produced no discernible change.

Similar results were obtained using the electromagnetic portion of the WAC calorimeter. A similar study was carried out using the modules in the FWD calorimeter. Again, as a function of E_t in the "global" triggering region, the energy flows and multiplicity of modules firing appear to be similar for hN and hA interactions.

CONCLUSIONS

The production of events with large amounts of E_t using nuclear targets is greatly enhanced over hydrogen. The majority of these events not jet-like. The yield enhancement increases faster than the number of nucleons within a nucleus. There is evidence that when "jet-like" events are produced, the enhancement varies as the number of nucleons in the nucleus, indicating a hard scattering mechanism.

To see if the enhancement is due to multiple scattering within the nucleus, correlations between the amount of energy in the central region and the energy detected in the target fragmentation region were studied. From these studies it appears that high E_t nA events are produced by multiple collisions within the nucleus.

The events from hydrogen and nuclear targets have similar event structure (multiplicity, energy flow) when events with similar E_t values are compared. It appears that the method by which E_t is produced (single vs. multiple collisions) is of secondary importance. This suggests that E_t may be a relevant parameter needed to describe the production of events.

REFERENCES

- 1) Otterlund, I., Nucl. Phys. A418, 87c (1984);
Busza, W., Acta. Phys. Pol. B8, 333 (1977)
- 2) Elias, J., et al., Phys. Rev. D22, 13 (1980)
- 3) De Marzo, C., et al., Phys. Rev. D26, 1019 (1982)
De Marzo, C., et al., Phys. Rev. D29, 2476 (1984)
- 4) For a review of quark-gluon plasma see topics "Quark Matter '84",
ed. Kajantie, K., Lecture Notes in Physics 221, Springer Verlag,
1985
- 5) Busza, W. and Goldhaber, A.S., Phys. Lett. 139B, 235 (1984)
- 6) Barton, D. et al., Phys. Rev. D27, 2580 (1983).
- 7) "Valence quark effects in beam remnants in high E_t pp collisions
at $\sqrt{s} = 27.4$ GeV", submitted to Phys. Rev. D.
- 8) Carrol, A. S., et al., Phys. Lett. 80B, 319 (1979)
- 9) Brown, B., et al., Phys. Rev. Lett. 50, 11 (1982);
Bromberg, C., et al., Phys. Rev. Lett. 42, 1202 (1979);
Bromberg, C., et al., Nucl. Phys. B171, 38 (1980);
- 10) Cronin, J., et al., Phys. Rev. D11, 3105 (1975);
Kluberg, L., et al., Phys. Rev. Lett. 38, 670 (1977);
Antreasyan, D., et al., Phys. Rev. D19, 764 (1979)
- 11) De Marzo, C., et al., Phys. Lett. 112B, 173 (1982);
De Marzo, C., et al., Nucl. Phys. B211, 375 (1983);
Brown, B., et al., Phys. Rev. Lett. 49, 711 (1982);
Brown, B. C., et al., Phys. Rev. D29, 1895 (1984)
- 12) Halliwell, C., Acta. Phys. Pol. B12, 141 (1981)